Article

Study of the properties of a composite material Fe$_{78}$Si$_9$B$_{13}$ / GNP in an epoxy matrix

Pagnola M.R^{1,3,*} , **Useche J.^{2}, Faig J.^{1,4}, Ferrari S.^{3} and Martínez García R.^{1}**

1   Instituto de Tecnologías y Ciencias de la Ingeniería, Universidad de Buenos Aires, Buenos Aires, Argentina.
2   Facultad de Ingeniería, Universidad Tecnológica de Bolívar, Cartagena, Colombia.
3   Departamento de Física, Universidad de Buenos Aires, Buenos Aires, Argentina.
4   Departamento de Ingeniería Mecánica, Universidad de Buenos Aires, Buenos Aires, Argentina.
*   Correspondence: mpagnola@gmail.com or mpagnola@fi.uba.ar

Abstract: This study investigates the properties of a composite material obtained by mixing Fe$_{78}$Si$_9$B$_{13}$ metallic powders (at %) with graphene nanoplates (GNP) in an epoxy matrix. Four composite types were created with GNP weight proportions of 0%, 0.5%, 1.0%, and 1.5%. The composites were embedded in transparent epoxy with weight proportions of 10%, 15%, and 20%, and then filled into 7 x 20 mm cylindrical probes. Twelve samples were prepared, and another 12 samples were subjected to a longitudinal magnetic field of 1 kG. All samples were tested with a Universal Testing Machine (Model WDW 10E) up to a maximum force of 20 kN. The experiment recorded deformation (ΔH) vs. load force. Most samples showed a maximum compression resistance of 390 MPa, except for a few that did not exceed 100 MPa. The magnetically oriented samples showed a greater elastic limit in the range of 200 to 270 MPa. Optical microscopy was used to observe the ordering of the particles after the application of the magnetic field. Scanning electron microscopy, energy dispersive X-ray spectroscopy, and X-ray diffraction were used to characterize the structure of the composite components. A vibrating sample magnetometer (VSM) was used to characterize the magnetic behavior of the metallic powders in the composite.

1. Introduction

The application range of soft magnetic materials such as Fe$_{78}$Si$_9$B$_{13}$ has been significantly increased due to the development of amorphous and nano-crystalline systems [1, 2]. Since then there has been interest in creating ferromagnetic alloys by rapid quenching of non-crystalline solids[3, 4]. The subsequent use of these materials in the fabrication of cores of electric transformers demonstrated a significant improvement in their overall performance, with a lower associated environmental impact as well. The manufacture of nanostructured magnetic packages, for various applications, can be carried out by using

metallic ribbons obtained by a melt spinning process. On the other hand, the epoxy is a material has a high degree of crosslinking and that make very interesting in term of high rigidity and strength. This makes it a candidate to perform a polymer-graphene based nanocomposite with low filler fractions. Fact that has managed to develop incipient investigations [5]. The high elastic modulus, high strength, and large specific surface area of graphene nanoplates (GNP) make them excellent nanofillers in the manufacture of metallic nanocomposites [6, 7]. Only the presence of graphene can improve the mechanical and electrical strength of the base material, allowing the development of materials with improved properties. However, the introduction of a third component in the matrix could provide complementary properties. This novelty has driven the development of the most varied composites, with an excellent combination of mechanical, electrical, and thermal properties [8]. The present work explores the development of a new composite material obtained by the homogeneous mixing of $Fe_{78}Si_9B_{13}$ metallic powders (at. %) with GNP, mixture which was embedded in an epoxy matrix to identify their different properties. The individual materials are also analyzed by X-ray diffraction (XRD), scanning electron microscopy (SEM), and electron energy-dispersive X-ray spectroscopy (EDX) for their structural and morphological characterization. The magnetic properties of the ribbons incorporated into the composite were obtained by a vibrating sample magnetometer (VSM).

2. Experimental Section

2.1. Preparation of Magnetic Particles

Soft magnetic ribbons of composition $Fe_{78}Si_9B_{13}$ (at. %) were used, obtained according to the procedures explained in Pagnola et al. [4] from a molten ingot in an induction furnace. Right after, by applying a mechanical milling treatment on the same, a powder was obtained as the raw magnetic material. The milling was performed in a ball mill that allows the frequency to be varied to process the sample. Prior to mechanical milling, a thermal treatment at 300°C for 2 hours [2], was performed on the as cast obtained ribbon to obtain a smaller particle size. Then, with the thermally treated ribbons, and at a frequency of 37.5 Hz, it was subjected to 1 hour of mechanical milling. This resulted in particles with a characteristic size of about 30 μm [9].

2.2. Preparation of GNP

Graphene was synthesized using a PM100 Retsch® planetary ball mill according to the procedure explained at reference [6]. For this, 5.0 g of commercial graphite (synthetic graphite powder with 99.9% purity, mesh No. 100) and 11.2 g of dry ice were used in the milling chamber of the planetary ball mill with 40 stainless steel balls of 12.7 mm in diameter and a volumetric hardness of 65 HRC for the process. The precursors were milled at 500 rpm for 24 h with the container sealed and fixed in the planetary ball mill. Subsequently, the internal pressure accumulated in the milling container was very slowly released. Since, when opening the lid of the container in a normal atmosphere, a set of sparks occurred, due to the hydration of the carboxylates into carboxylic acids in the atmospheric humidity [10]. Once the process was finished, the samples were carefully extracted from the milling chamber and transferred to an Erlenmeyer flask, washed with 15% hydrochloric acid to dissolve and remove all iron impurities from the balls. Finally, the samples were filtered and washed with distilled water. Then they were dried at 60°C and stored for their subsequent characterization.

2.3. Preparation of Powder Mixtures

Four samples were prepared to characterize their magnetic behavior: a sample consisting entirely of $Fe_{78}Si_9B_{13}$ magnetic particles after mechanical milling, a sample consisting of a mixture of $Fe_{78}Si_9B_{13}$ magnetic particles after mechanical milling with 0.5% by weight of graphene nanosheets, a sample consisting of a mixture of $Fe_{78}Si_9B_{13}$ magnetic particles after mechanical milling with 1% by weight of graphene nanoplates, and a sample consisting of a mixture of $Fe_{78}Si_9B_{13}$ magnetic particles after mechanical milling with 1.5% by weight of graphene nanosheets. All graphene nanoplates used were obtained according to Section 2.2. Each of the mixtures obtained was placed for about 45 minutes under low frequency conditions (below that of the one used in mechanical milling) within separate milling vessels but without balls. In this way, it was possible to homogenize the low energy mixing of all the powder material, avoiding affecting the particles individually, modifying their structure, or contributing metallic charge residues (from the balls) to the mixed particles. Likewise, a homogeneous distribution was achieved in the powder material of the composite. These four powder samples obtained were characterized magnetically in their behavior for the present work.

2.4. Obtaining the Composite for the Samples

The composite of the samples was constituted by epoxy material and the metallic powders detailed in Section 2.1 with the graphene nanoplates obtained according to Section 2.2 according to the procedure explained in Section 2.3. The nomenclature of the samples for our composite is "X-Y-(sO, O)", where X is the weight percentage of GNP; Y is the percentage of $Fe_{78}Si_9B_{13}$ in the polymer epoxy matrix. All samples were obtained in two different large batches, one of them determines the non-directional samples (sO) and the other the directional ones (O). The latter, obtained in had-hoc device with an external magnetic field of 1 kG applied during the polymerization of the epoxy, according to the scheme of Figure 1. In this way, a total of 24 samples with different proportions of GNP and metallic powders of $Fe_{78}Si_9B_{13}$ in the matrix of epoxy material followed the proportions shown in Table 1. The epoxy material used is the commercial two-component one (Similar to D.E.R.® 331 EPOXY RESIN) with a proportion of 50% Wt. of each for all samples and possesses an ultimate tensile strength (UTS) of 10.8 MPa according to ASTM D1002 norm [11]. The cylinder probes obtained have dimensions of 7 x 20 mm (diameter x length).

Table 1. Values of weight percentage of the components used in the probes of the samples fabricated.

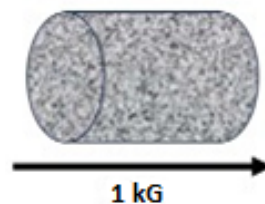| % Weight of GNP	% Weight of $Fe_{78}Si_9B_{13}$ powder	Type of batch
0; 0.5; 1 y 1.5	10; 15; 25	O; sO

Figure 1. Scheme of the application of an external magnetic field in a longitudinal way on the samples that will acquire a preferential orientation.
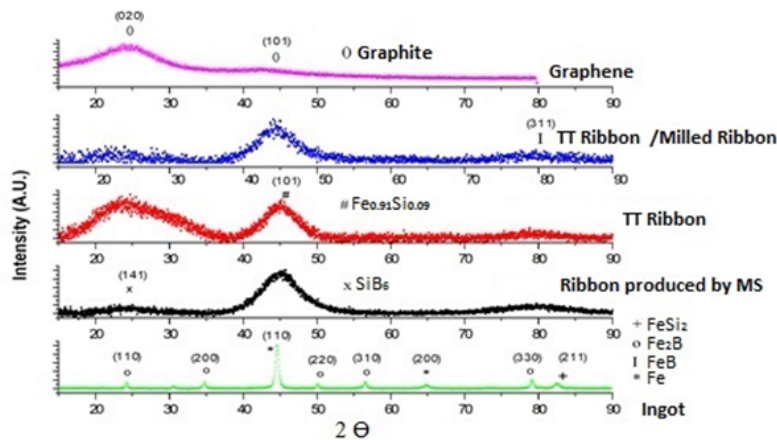
Figure 2. Characteristic diffractograms of original and heat-treated components.

3. Characterization of the components

The (XRD) X-ray diffraction characterization was carried out by Rigaku instrument with a $\theta - 2\theta$ goniometer configuration employing Cu-K$_\alpha$ radiation ($\lambda = 0.15418$ nm). The ribbons obtained from an original ingot exhibits a predominantly amorphous structure, except for the FeSi-rich peak at (1 0 1) with a nanocrystalline grain size of 1.6 ± 0.4 nm. In thermally treated ribbons, there is an increase in the intensity of the pre-peak compared to untreated ribbons. The size of the nanocrystalline phase rich in FeSi in thermally treated ribbons increases to 2 nm. The increase in the (1 4 1) peak corresponds to the segregation of the SiB$_6$ nanocrystalline phase. Meanwhile, the (1 0 1) and (3 1 1) peaks exhibit a marginal decrease in their relative heights due to the thermal treatment applied to the ribbons [2, 9, 10, 12].

Table 2. Correspondance phases of the crystallographic planes (found in XRD) of the ribbons of Fe$_{78}$Si$_9$B$_{13}$.

Element	Peak	Record # in ICSD	Reference
SiB$_6$	(1 4 1)	#35-0809	[13]
Fe$_{0.91}$Si$_{0.09}$	(1 0 1)	#96-900-6909	[14]
FeB	(3 1 1)	#32-0463	[15]

The as cast ingot, on the other hand, exhibits a crystalline structure in all its peaks (Figure 2 – ingot), which, in conjunction with the alloy's stoichiometry, indicates the presence of Fe$_2$B, FeSi$_2$, and Fe [2]. The composition of the ribbons produced by melt spinning was characterized using a ZEISS EVO 10 scanning electron microscope equipped (See Table 2) with an Oxford Instruments Ultim Max 40 Silicon Drift Detector (SDD) [2].

Additionally, the overall chemical composition of the magnetic ribbon was determined in a sufficiently representative area through Energy Dispersive X-ray Spectroscopy (EDX), yielding the compositional analysis presented in Table 3.

The graphene characterization in Figure 2 reveals the presence of two diffraction peaks at 23.78° and 44.3°, corresponding to the crystallographic planes (0 2 0) and (1 0 1) associated with graphite. This is attributed to the fact that graphene retains the atomic structure of carbon atoms after the mechanical

Table 3. Compositional analysis by EDX of the metallic ribbons produced by melt spinning.

| Element	% wt.	Sigma % wt.	% at.
B	2.48	0.84	11.09
Si	5.30	0.07	9.11
Cr	0.11	0.03	0.10
Fe	92.11	0.80	79.70

exfoliation process [16]. The number of stacked nanoplates in the GNP was determined following the procedure outlined by Pagnola et al. [9] and is detailed in Table 4.

Table 4. Characterization of GNP.

Material	$2\Theta_{max}$	D (nm)	d (nm)	NI
Graphene	23.78	0.37	2.22	6

The magnetic behavior of the mixtures used for obtaining the composites was studied in a VSM at a very low frequency up to a magnetic field of 20000 Oe. With this equipment, the magnetic response of the samples was obtained.

It can then be stated that the saturation magnetization (Ms) decreases with the addition of GNP to the mixture, with the highest value within the composites being that of the mixture with 0.5% by weight of GNP, with 143 emu/g. This value decreases by 10 emu/g when it reaches 1.5% by weight. On the other hand, the behavior with the coercivity of the samples is more erratic, as there is no clear trend in this according to the addition of GNP to the mixture (see Figure 3) [9].
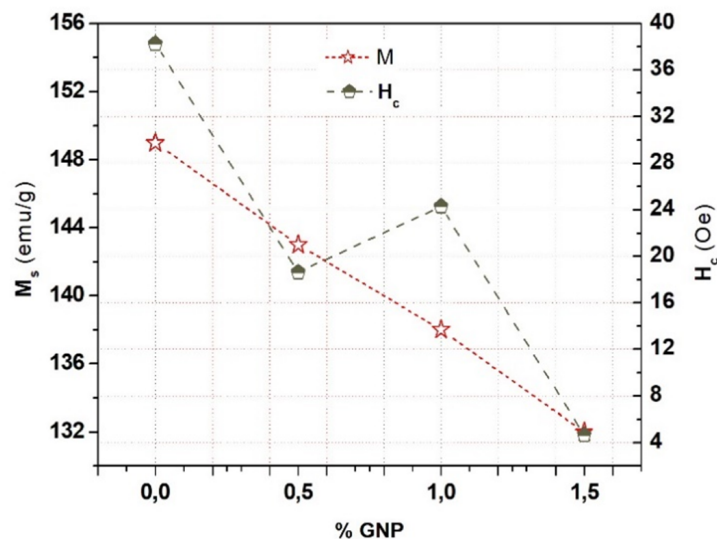
Figure 3. Values of the saturation magnetization (Ms) and Coercive Field (Hc) for $Fe_{78}Si_9B_{13}$ samples with GNP.
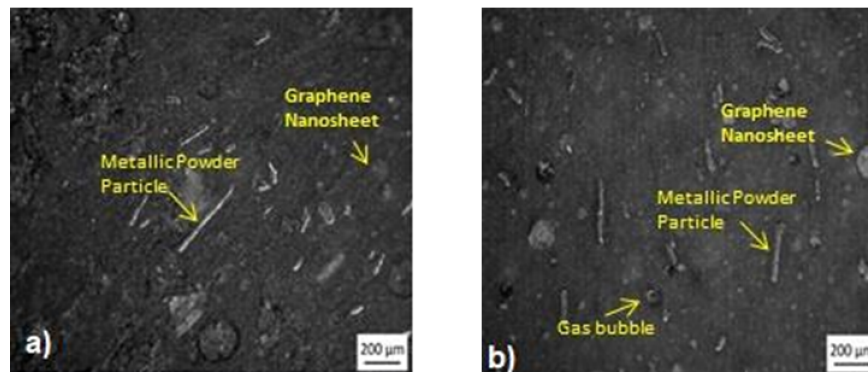
Figure 4. Optical micrographs of the powder material embedded in epoxy a) Sample 0-25-sO: without GNP powder of $Fe_{78}Si_9B_{13}$ mixed in 25 weight% in the epoxy matrix and without preferential orientation; b) Sample 0-10-O: without GNP powder de $Fe_{78}Si_9B_{13}$ mixed in 10 weight % in the epoxy matrix with preferential orientation.

4. Results and discussion

4.1. Results

Over both groups of samples (sO and O), cross-section cuts were made, to allow the distribution of particles in volume to be characterized observationally by optical microscopy. In contrast, the batch with preferential orientation (O) shows a more ordered behavior in its distribution, generated by the external magnetic field applied during the drying process (Figure 4b).

Two groups of particles can be observed, some elongated, corresponding to the $Fe_{78}Si_9B_{13}$ metallic powders, and others in the form of plates or planes that are present in a smaller proportion and correspond to the graphene nanosheets in the mixture. Figure 4 depicts the characteristics obtained, which are principally the randomness in the distribution corresponding to the batch of samples without preferential orientation (sO) (see Figure 4a). Also, traces of gas bubbles can be observed in the lower central part of Figure 4b, on the epoxy matrix. Which corresponds to the release of gases occluded between particles during the alignment process by the application of the external magnetic field. This phenomenon is observed throughout the group of samples obtained with preferential orientation and is distinctive in this batch.

To obtain structural parameters of the samples, both groups of specimens are subjected to a compression test in a Universal Testing Machine WDW 10E with a displacement rate of 0.5mm/min. To do this, the samples are placed between both compression plates according to Figure 5.

Figure 5. Scheme of the samples for the compression tests.

4.2. Discussion

4.2.1. Samples without graphene oxide nanoplates

The mechanical properties of the composite are determined by the properties of the materials that are the parts of it, and also by the microstructure of the sample. Figure 6 shows the compression curves corresponding to the series of samples of the composite material tested. In these composites, no graphene (no GNP) was added. The $Fe_{78}Si_9B_{13}$ particles have a thickness on the order of the micron, and a sheet-like shape. This shape affects the way in which the particles are distributed in the polymer matrix under the effect of the magnetic field. With a polymerization of the epoxy resin under an external magnetic field, the $Fe_{78}Si_9B_{13}$ particles orient themselves in the direction of the field and a preferential direction of ordering of them is established in the epoxy matrix. When the magnetic field is absent in the polymerization process, the particles are distributed randomly in the polymer matrix.

All samples were subjected to the same compressive load. The values of force applied to the specimens affect the polymeric component of the composite more because they are atomic chains of light atoms, with relatively weak atomic bonds. The $Fe_{78}Si_9B_{13}$ particles are a more compact material, with strong atomic bonds, and metallic properties of ductility and malleability. The elastic module for these samples is established in Table 5.
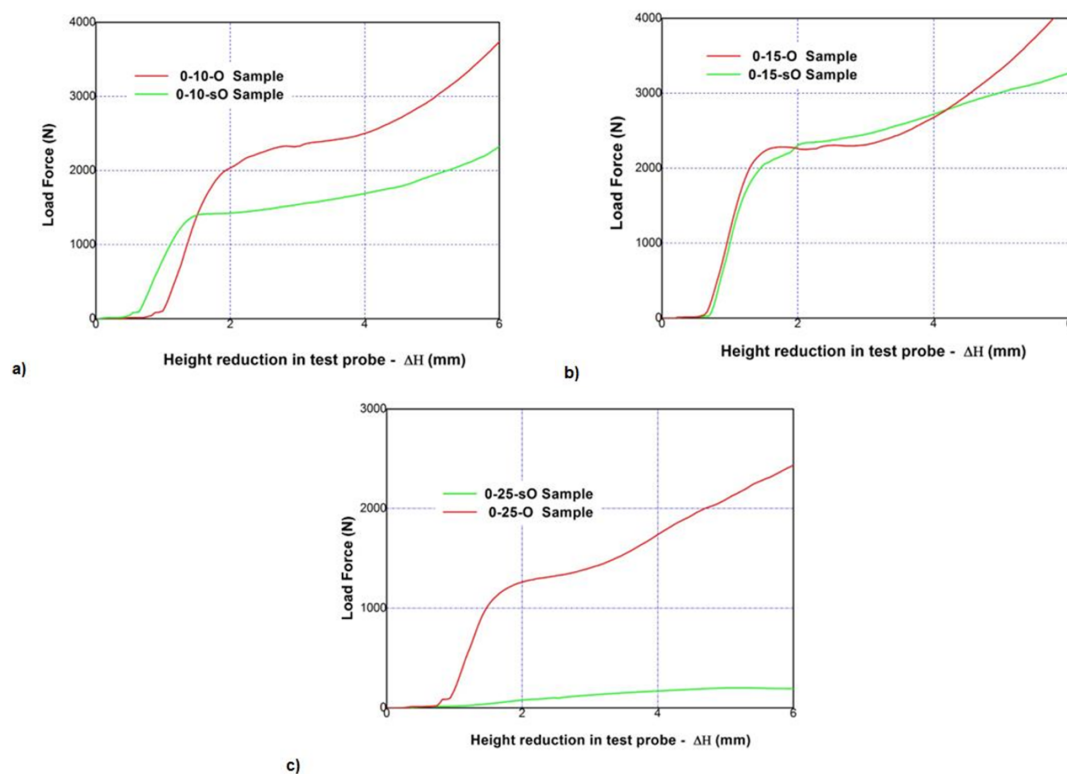

Figure 6. Compression curves corresponding to a set of samples of composite material made of epoxy and particles of $Fe_{78}Si_9B_{13}$ without (sO) and with orientation (O) due to an external magnetic field applied in the lapse of the polymerization of the epoxy. a) 0-10-O and 0-10-sO samples; b) 0-15-O and 0-15-sO samples; c) 0-25-O and 0-25 sO samples. (There are no graphene nanoplates in these probes).

Table 5. Young's elastic modulus (E) of samples without GNP.

Sample	E (MPa)	
	sO	O
0-10	443.2	509.8
0-15	699.5	676.7
0-25	12.5	376.1

The curves in Figure 6 can be interpreted as the way the $Fe_{78}Si_9B_{13}$ particles in form of sheets reinforce the composite material, and how they do so depending on whether or not they are oriented in a preferential direction. In the same figure, it can be observed that the amount of $Fe_{78}Si_9B_{13}$ particles dispersed in the polymer matrix increases from 10% to 25%. In all cases, the resistance to compression deformation is greater when the particles are oriented preferentially in the matrix. This behavior is maximized in the case of composites formed by 25% $Fe_{78}Si_9B_{13}$ particles dispersed in the polymer. In this case, the samples deform 5 mm under a force of about 200 N when the particles are randomly distributed and under a force of about 2000 N when they are oriented preferentially. This means that 10 times more force is required to produce the same deformation. This can be explained by the difference in microstructure that exists between the two types of samples (see Figure 4). The composite formed by $Fe_{78}Si_9B_{13}$ particles in sheet form that orient in an easy magnetization axis under the action of an external magnetic field has a highly ordered and anisotropic microstructure in terms of the measured property. This anisotropy due to the microstructural order manifests itself in a direction in space that has more resistance to mechanical deformation.

4.2.2. Samples with graphene nanoplates

These samples were obtained in a similar way to those reported in Figure 6, but with amounts of graphene oxide between 0.5% and 1% weight. When GNP particles are added, the composite behavior materials change. There is no longer a significant difference between the behavior of samples with oriented and non-oriented $Fe_{78}Si_9B_{13}$ particles (less than a 30% variation from reported values). The Figure 7 shows compression curves corresponding to the composite material with different amounts of graphene oxide particles added to the epoxy and $Fe_{78}Si_9B_{13}$ mixture. In all cases, it is observed that the difference in the force value required to cause a deformation of 4 mm in the composites oscillates between 5% and 23% regardless of whether the $Fe_{78}Si_9B_{13}$ particles are oriented or not (see Figure 7). This is a significant difference from the behavior shown by composites without GNP, where these differences (in the elastic module) are up to 10 times higher (see Figure 6).

The similarity in the mechanical behavior of composites with oriented and non-oriented $Fe_{78}Si_9B_{13}$ particles that have GNP added may be due to the fact that an adding graphene particle does not help to establish a preferential orientation. An associated microstructural order is also not reached with this. Graphene and $Fe_{78}Si_9B_{13}$ particles are mechanically mixed before being added to the epoxy resin, so each magnetic particle is near to non-magnetic GNP. This causes the $Fe_{78}Si_9B_{13}$ magnetic particles to have to overcome greater resistance from their microstructural environment in order to align themselves in the direction of the applied magnetic field. The result is a less efficient preferential orientation and a less ordered microstructure than in the case of the absence of GNP in the composite. This can be seen in Figure 8, where it can be seen that an efficient preferential orientation of the $Fe_{78}Si_9B_{13}$ particles is not achieved when GNP is added, and the microstructure of the composites obtained, with and without applied magnetic field, is similar. Since the microstructure of the obtained composites is similar, therefore the mechanical properties also are also similar when comparing the elasticity modulus (see Table 6).
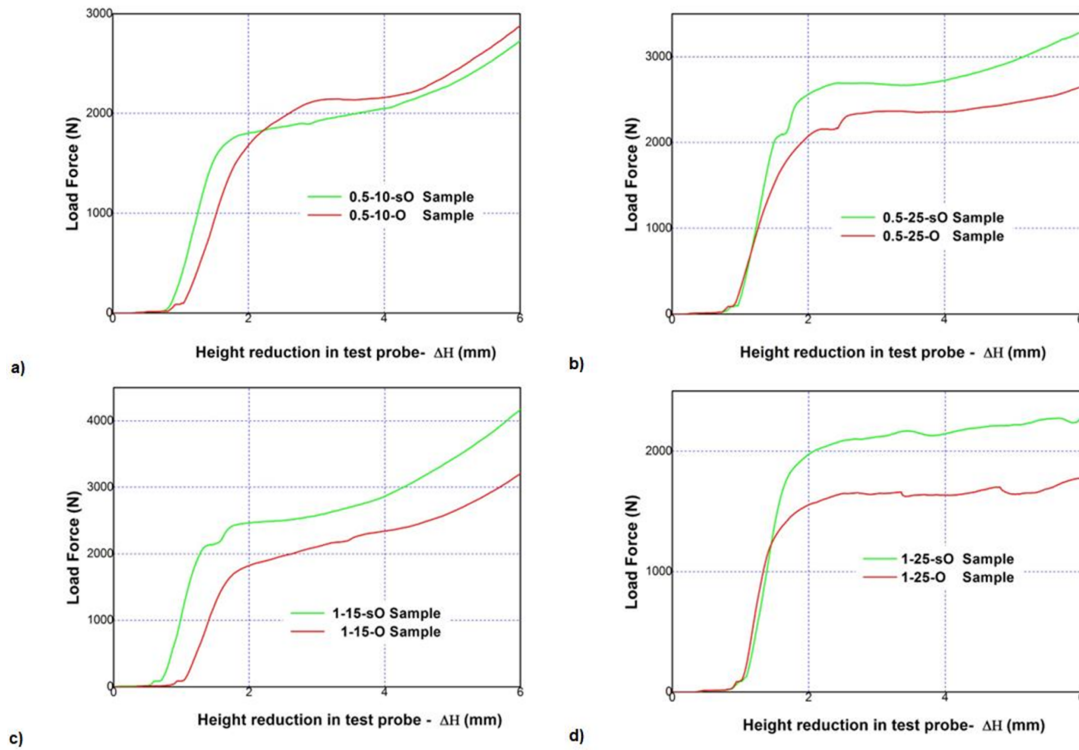
Figure 7. Samples with different amounts of graphene particles in the composite. Material composed of epoxy, graphene particles, and non-oriented $Fe_{78}Si_9B_{13}$ particles oriented with an external magnetic field during the polymerization of the epoxy. a) 0.5-10-O and 0.5-10-sO samples; b) 0,5-25-O and 0.5-25-sO samples; c) 1-15-O and 1-15-sO samples; d) 1-25-O and 1-25-sO samples.

Table 6. Young's elastic modulus (E) of samples with graphene nanoplates.

Sample	E (MPa)	
	sO	O
0.5-10	604.1	476.5
0.5-25	725.5	515.2
1-15	679	505.4
1-25	811	618.4

The 1-15-sO sample supports a greater applied force with less displacement, i.e., it has a higher stiffness. In contrast, the 0-25-sO sample has the lowest structural stiffness of the set of non-oriented samples. In contrast, it is evident that the 0-15-O sample has the best structural stiffness compared to the 1-25-O sample, which shows greater deformation with a lower applied load. In samples without GNP, higher structural stiffness is observed for the batch with preferential orientation (O) in min-max GNP extremes percentage used in powdered material (10, 25% by weight). The opposite can be said for samples with 0.5 to 1% GNP added. That is to say, the non-oriented samples (sO) have better structural stiffness behavior. With the addition of 1.5% GNP, the structural stiffness of samples with preferential orientation (O) seems to decrease too for all percentages of powdered material used in the composite. Up to 4 mm in deformation of the specimen, the greatest elastic limits reached are for samples with preferential orientation (O) and GNP incorporated. Reaching close values to 115 and 270 MPa. Except for sample 0.5-25 with a value close to
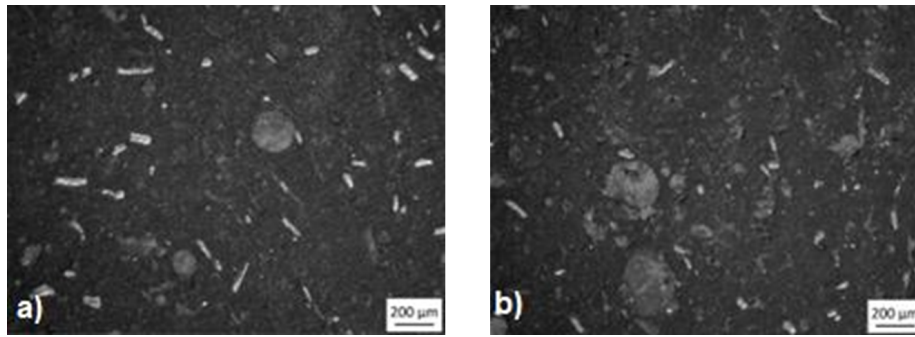
Figure 8. a) Optical micrograph of sample 1-25-sO, b) Optical micrograph of sample 1-25-O. (No great microstructural difference is observed).

116 MPa. On the other hand, the samples without GNP show greater rigidity for (sO) batch, except for the sample 0-15-O which shows a greater rigidity near to 117 MPa (See Table 7). The probes 0.5-15-sO; 1-10-sO; 1.5-10-sO and 1.5-25-sO reached a lower resistance to tension respect the rest of the samples.

Table 7. Values of Elastic Limit and Compression Tension required to deform 4 mm of the probe.

Sample	Elastic Limit (MPa)		Compression tension (MPa)	
	sO	O	sO	O
0-10	211.61	195.98	33.5	50.2
0-15	89.71	117.54	54.4	53.0
0-25	273.5	235.74	3.42	34.6
0.5-10	117.59	274.75	40.8	43.1
0.5-15	34.36	195.76	—	49.0
0.5-25	270.82	115.94	54.4	46.8
1-10	63.82	272.38	14.0	45.4
1-15	125.45	156.42	57.2	46.7
1-25	115.88	272.75	42.6	32.6
1.5-10	41.33	272.78	46.0	49.0
1.5-15	192.02	123.48	49.1	41.1
1.5-25	40.34	196.13	42.4	34.5

5. Conclusions

The mechanical properties of the composite are determined by the properties of the materials that compose it and by the microstructure of the sample. For all samples, the mechanical tests show a linear behavior in the first stages of deformation due to the elastic properties of the epoxy, followed by a flow behavior and a third stage of hardening associated with the compaction of the specimen. The mechanical behavior of the samples is affected by the percentage of $Fe_{78}Si_9B_{13}$ powder and whether it appears distributed randomly or oriented in the material. As the amount of $Fe_{78}Si_9B_{13}$ powder increases, ductility decreases due to an increase in brittleness and the generation of microfactures. This effect is greater when the $Fe_{78}Si_9B_{13}$ powder is randomly distributed in the material (without preferential orientation). The preferential orientation of the $Fe_{78}Si_9B_{13}$ particles affects the mechanical properties of the composite. This effect is more notable for higher percentages of $Fe_{78}Si_9B_{13}$ powder. The value of Young's Modulus changes little in the case of oriented or non-oriented particles when the percentages of $Fe_{78}Si_9B_{13}$ in the composite are 10% and 15% by weight of the composite, however, the change is notable for a percentage of

25% in weight. In this case, a difference of up to 30 times is observed in Young's Modulus value between composites with $Fe_{78}Si_9B_{13}$ particles oriented and not oriented in a preferential direction. This behavior may be due to the fact that there is a critical quantity of oriented particles in the volume from which each differential (element) of the sample volume supports the applied stress more homogeneously. When the amount of $Fe_{78}Si_9B_{13}$ particles with preferential orientation is lower (10%, 15%), the stress is distributed in the polymer matrix with few interactions with the oriented particles because they are few in volume. This behavior changes when the microstructure of the composite is modified by adding graphene oxide particles as a dopant. By adding graphene, the Young's Modulus value changes appreciably (up to 30% of the value) between composites with oriented and unoriented $Fe_{78}Si_9B_{13}$ particles. This occurs regardless of the percentage of $Fe_{78}Si_9B_{13}$ particles in the sample. Such behavior may be due to the fact that the graphene oxide particles in the volume of the composite obstruct the $Fe_{78}Si_9B_{13}$ particles so that they can rotate and orient themselves in the direction of the magnetic field that seeks to orient them. As result the microstructure of all the samples is similar since in no case are the $Fe_{78}Si_9B_{13}$ particles oriented efficiently. Taking the above into account, to obtain structural improvements and not interfere in the preferential arrangement of the $Fe_{78}Si_9B_{13}$ particles, it would be advisable not to add more than 1% by weight of graphene oxide particles to the composite.

Acknowledgments

Disclosure statement: The authors declare no conflict of interest. The funders had no role in the design of the study; in the collection, analyses, or interpretation of data; in the writing of the manuscript; or in the decision to publish the results.

References

[1] Fabiana Morales, Marcelo Pagnola, Juan Muriel, and Leandro Socolovsky. Molienda mecánica sobre cintas magnéticas blandas de fe78si9b13 con molino de bolas ortorrómbico de fabricación propia. *Revista SAM N°1*, page 61–67, 2020.

[2] Da-guo Jiang and Zhao-hui Liu. Preparation and piezomagnetic effect of FeSiB amorphous powders /IIR composite film. *In 2010 Third International Symposium on Intelligent Information Technology and Security Informatics*, pages 268–270, 2010.

[3] M. Pagnola, M. Malmoria, and M. Barone. Biot number behaviour in the chill block melt spinning (cbms) process. *Applied Thermal Engineering*, 103:807–811, 2016.

[4] Marcelo R. Pagnola, Mariano Malmoria, Marcelo Barone, and Hugo Sirkin. Analysis of fe78si9b13 (*Multidiscipline Modeling in Materials and Structures*, 10(4):511–524, Nov 2014.

[5] N I C Berhanuddin, I Zaman, S A M Rozlan, M A A Karim, B Manshoor, A Khalid, S W Chan, and Q Meng. Enhancement of mechanical properties of epoxy/graphene nanocomposite. *Journal of Physics: Conference Series*, 914(1):012036, oct 2017.

[6] M. R. Pagnola, F. Morales, P. Tancredi, and L. M. Socolovsky. Radial Distribution Function Analysis and Molecular Simulation of Graphene Nanoplatelets Obtained by Mechanical Ball Milling. *JOM*, 73(8):2471–2478, jan 2 2021.

[7] MA Wenshi, Zhou Junwen, and Cheng Shunxi. Preparation and characterization of graphene. *Journal of Chemical Engineering of Chinese Universities*, 24(4):719–722, 2010.

[8] J. Kováčik and Š. Emmer. Cross property connection between the electric and the thermal conductivities of copper graphite composites. *International Journal of Engineering Science*, 144:103130, 11 2019.

[9] M. Pagnola, J. Useche V., and R. Martinez García. Obtención de Fe78Si9B13/GNPL composite: Un estudio de propiedades. *21st LACCEI International Multi-Conference for Engineering, Education, and Technology, (Buenos Aires, Argentina).*, jul 18 2023.

[10] I. Y. Jeon, Y. R. Shin, G. J. Sohn, H. J. Choi, S. Y. Bae, J. Mahmood, S. M. Jung, J. M. Seo, M. J. Kim, D. Wook Chang, L. Dai, and J. B. Baek. Edge-carboxylated graphene nanosheets via ball milling. *Proceedings of the National Academy of Sciences*, 109(15):5588–5593, mar 27 2012.

[11] D14 Committee et al. Test method for apparent shear strength of single-lap-joint adhesively bonded metal specimens by tension loading (metal-to-metal). *ASTM International*, 2019.

[12] Y. Dong, Z. Li, M. Liu, C. Chang, F. Li, and X. M. Wang. The effects of field annealing on the magnetic properties of FeSiB amorphous powder cores. *Materials Research Bulletin*, 96:160–163, 12 2017.

[13] MC MORRIS, HF MCMURDIE, EH EVANS, B PARETZKIN, HS PARKER, NP PYRROS, and C HUBBARD. Standard x-ray diffraction power patterns: Section 20- data for 71 substances[final report]. 1984.

[14] J. Zhang and F. Guyot. Thermal equation of state of iron and $Fe_{0.91}Si_{0.09}$. *Physics and Chemistry of Minerals*, 26(3):206–211, 1999.

[15] CR Hubbard. Standard x-ray diffraction powder patterns: section 18—data for 58 substances. *National Bureau of Standards Monogr*, 1981.

[16] G. Huang, C. Lv, J. He, X. Zhang, C. Zhou, P. Yang, Y. Tan, and H. Huang. Study on Preparation and Characterization of Graphene Based on Ball Milling Method. *Journal of Nanomaterials*, 2020:1–11, 2020.